Preprint typeset in JHEP style - HYPER VERSION

FERMILAB-PUB-07-274-A-T
October 3, 2007

arXiv:0706.3409v2 [hep-ph] 4 Oct 2007

Spinless photon dark matter from two universal extra dimensions

Bogdan A. Dobrescu[1], **Dan Hooper**[2], **Kyoungchul Kong**[1], **Rakhi Mahbubani**[1]

[1] *Theoretical Physics Department, Fermilab, Batavia, IL 60510, USA*
[2] *Theoretical Astrophysics Department, Fermilab, Batavia, IL 60510, USA*
bdob@fnal.gov, dhooper@fnal.gov, kckong@fnal.gov, rakhi@fnal.gov

Abstract: We explore the properties of dark matter in theories with two universal extra dimensions, where the lightest Kaluza-Klein state is a spin-0 neutral particle, representing a six-dimensional photon polarized along the extra dimensions. Annihilation of this 'spinless photon' proceeds predominantly through Higgs boson exchange, and is largely independent of other Kaluza-Klein particles. The measured relic abundance sets an *upper* limit on the spinless photon mass of 500 GeV, which decreases to almost 200 GeV if the Higgs boson is light. The phenomenology of this dark matter candidate is strikingly different from Kaluza-Klein dark matter in theories with one universal extra dimension. Elastic scattering of the spinless photon with quarks is helicity suppressed, making its direct detection challenging, although possible at upcoming experiments. The prospects for indirect detection with gamma rays and antimatter are similar to those of neutralinos. The rates predicted at neutrino telescopes are below the sensitivity of next-generation experiments.

Contents

1. Introduction **1**

2. Spinless photon annihilation **3**
- 2.1 Annihilation into boson pairs 4
- 2.2 Annihilation into fermion pairs 6

3. Relic abundance **8**
- 3.1 From annihilation cross sections to relic abundance 9
- 3.2 Prediction for the spinless photon mass 10

4. Astrophysical Detection **12**
- 4.1 Direct Detection 12
- 4.2 Indirect detection 14

5. Conclusions **16**

1. Introduction

Theories with universal extra dimensions [1] have a Z_2 symmetry, which is a remnant of invariance under translations along the compact dimensions. This Z_2 symmetry, usually called Kaluza-Klein (KK) parity, implies that the lightest KK particle is stable, and a potentially viable dark matter candidate.

In the case of a single universal extra dimension compactified on an interval, the geometrical origin of KK parity is the invariance under reflections with respect to the center of the interval. A one-loop computation of the mass splitting between KK particles shows that the lightest KK particle is typically the level-1 mode of the hypercharge gauge boson [2]. It turns out that this is an attractive dark matter candidate [3, 4, 5], whose relic abundance is consistent with the observed dark matter density for a mass between 500 GeV and about 1.5 TeV, as shown by detailed computations including coannihilations [6] and level-2 resonances [7]. Direct detection of this KK dark matter is possible with next generation experiments [4, 8, 9], while indirect detection has somewhat better prospects than is found in the case of neutralinos [4, 10, 11, 12, 13]. Other dark matter candidates, such as the level-1 KK mode of the graviton or of a right-handed neutrino, are also viable for certain ranges of parameters in models with one universal extra dimension [14, 15, 16].

Theories with two universal extra dimensions (see Ref. [17] and references therein) also contain a KK parity. In the case of the simplest compactification that leads to chiral zero-mode fermions, a ('chiral') square with adjacent sides identified [18, 19], the KK parity transformations are reflections with respect to the center of the square. Momentum along the two compact dimensions is quantized such that any 6-dimensional field propagating on the square appears as a set of 4-dimensional particles labeled by two positive integers, (j, k). These particles are odd under KK parity when $j + k$ is odd, and are even otherwise. In any process, odd particles may be produced or annihilated only in pairs. The lightest odd particle, which is one of the (1,0) states, is thus stable.

Gauge bosons propagating in six dimensions may be polarized along the two extra dimensions. As a result, for each spin-1 KK particle associated with a gauge boson, there are two spin-0 fields transforming in the adjoint representation of the gauge group. One linear combination becomes the longitudinal degree of freedom of the spin-1 KK particle, while the other linear combination remains as a physical spin-0 particle, called the spinless adjoint.

The 6-Dimensional Standard Model (6DSM), in which the Standard Model fields and three right-handed neutrinos propagate in two universal extra dimensions compactified on the chiral square, has been described in Ref. [17]. Including one-loop corrections to masses in the 6DSM [20], the lightest (1,0) particle is a linear combination of the electrically-neutral spinless adjoints of the electroweak gauge group. This is essentially a photon polarized along the extra dimensions, which we will refer to as the 'spinless photon'. At colliders, (1,0) particles may be pair produced and then undergo cascade decays that end with spinless photons escaping the detector [21].

In this paper we study the viability of the spinless photon as dark matter, as well as the prospects for its detection. In the absence of majorana masses, the scalar nature of this dark matter candidate implies that its scattering cross sections with Standard Model fermions are suppressed, being proportional to the fermion mass. This is in contrast to the case of KK dark matter in one universal extra dimension, where the lightest KK particle has spin 1, which allows for a large annihilation cross sections to leptons. Nevertheless, the spinless photons may annihilate into W^+W^-, ZZ and Higgs boson pairs, and we will show that for a range of masses correlated with the Higgs mass, the relic abundance is consistent with the measured dark matter abundance. Although elastic scattering of spinless photons with nucleons is similarly helicity suppressed, its direct detection may be possible at next-generation experiments. The relatively small elastic scattering cross section leads to undetectable rates at neutrino telescopes. Furthermore, given that pairs of spinless photons annihilate into heavy Standard Model particles, their indirect detection with gamma rays and antimatter is somewhat more difficult than in the 5D case. We find that in most phenomenological respects, dark matter in the 6DSM more closely resembles a neutralino than KK dark matter in one universal extra dimension.

boson	MR	fermion	MR
$G_\mu^{(1,0)}$, $G_H^{(1,0)}$	1.39 , 1.00	$\left(T_+^{(1,0)}, B_+^{(1,0)}\right)$	$1.27 + \frac{1}{2}(m_t R)^2$
$W_\mu^{(1,0)3}$, $W_\mu^{(1,0)\pm}$	$1.06 + \frac{1}{2}(m_W R)^2$	$T_-^{(1,0)}$	$1.25 + \frac{1}{2}(m_t R)^2$
$\left(H^{(1,0)+}, H^{(1,0)0}\right)$	$1.05 + \Delta_h$	$\left(U_+^{(1,0)}, D_+^{(1,0)}\right)$	1.25
$\mathcal{G}_{\mu\nu}^{(1,0)}$, $B_\mu^{(1,0)}$	1.00 , 0.97	$U_-^{(1,0)}$, $D_-^{(1,0)}$	1.22 , 1.21
$W_H^{(1,0)3}$, $W_H^{(1,0)\pm}$	$0.92 + \frac{1}{2}(m_W R)^2$	$\left(N_+^{(1,0)}, E_+^{(1,0)}\right)$	1.04
$B_H^{(1,0)} \equiv B_H$	0.86	$E_-^{(1,0)}$, $N_-^{(1,0)}$	1.04 , 1.00

Table 1: Masses of the (1,0) particles in units of the compactification scale $1/R$. The (1,0) fermion masses are almost the same for all three generations, with the exception of the top-quark KK modes. The mass splittings depend on standard model couplings, and thus depend logarithmically on $1/R$. Here we used $1/R = 500$ GeV, and we kept only the leading terms in the $m_t R$ expansion, where m_t is the top-quark mass. The correction Δ_h to the (1,0) Higgs masses is unknown, being quadratically sensitive to the cutoff scale.

2. Spinless photon annihilation

The mass spectrum of (1,0) particles in the 6DSM [17], including the logarithmically enhanced one-loop corrections computed in Ref. [20], is detailed in Ref. [21]. The essential feature of that spectrum is that the spinless adjoint of the hypercharge gauge group, $B_H^{(1,0)}$ (labeled for brevity B_H in this paper), is the lightest (1,0) particle, and therefore a dark matter candidate.

There may be contributions from cutoff-scale physics to operators localized at the corners of the square compactification, which are invariant under KK parity and modify the mass spectrum [17]. In principle, these could turn some other (1,0) particle into the lightest KK-odd state. Hence, the (1,0) modes of the graviton ($\mathcal{G}_{\mu\nu}^{(1,0)}$), of the right-handed neutrinos ($N_-^{(1,0)}$), of one of the electrically-neutral components of the Higgs doublet ($H^{(1,0)0}$) or of the electroweak bosons ($B_\mu^{(1,0)}$, $W_\mu^{(1,0)3}$, $W_H^{(1,0)3}$), could all be viable dark matter candidates. We leave the investigation of these possibilities for future work.

Electroweak symmetry breaking induces mixing between B_H and the electrically-neutral spinless adjoint of $SU(2)_W$, $W_H^{(1,0)3}$, so that it is appropriate to call B_H the spinless photon. However, this mixing is suppressed by $m_W R$, where m_W is the W boson mass, and $1/R$ is the compactification scale. For simplicity we will ignore mixing effects in what follows. This approximation is not valid if both M_B and the mass of $W_H^{(1,0)3}$ are below $\mathcal{O}(100)$ GeV. However, localized operators could increase the mass of $W_H^{(1,0)3}$ without changing M_B, so in the limit where $W_H^{(1,0)3}$ is much heavier than m_W our results apply to any value of M_B.

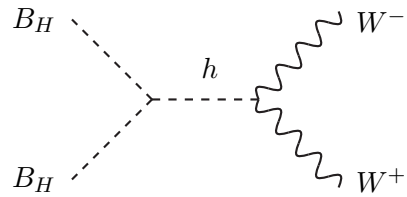

Figure 1: The only tree-level contribution to $B_H B_H$ annihilation into W^+W^-. The same diagram with the W bosons replaced by Z bosons describes annihilation into Z pairs.

As we will see in this section, the only other (1,0) particles that affect the annihilation cross section of B_H are the KK modes of the top quark: $T_-^{(1,0)}$, which is an $SU(2)_W$-singlet vectorlike quark, and $T_+^{(1,0)}$, which together with $B_+^{(1,0)}$ forms an $SU(2)_W$-doublet vectorlike quark. The masses of other (1,0) quarks are necessary for computing the elastic scattering cross section of B_H with nucleons (see Section 4). The masses of the (1,0) leptons and vector bosons are largely irrelevant for our present study. Nevertheless, we show in Table 1 the full (1,0) spectrum from Ref. [21], which turns out to include sufficiently large mass splittings so that coannihilation effects may be neglected. We loosely refer to all (1,0) particles as 'level-1' modes in what follows, and we label them using the superscript $(1,0)$.

2.1 Annihilation into boson pairs

The interaction of the B_H with the Standard Model Higgs boson, h, is given by

$$\mathcal{L}_h = -\frac{g_Y^2}{8} B_H B_H h\,(h+2v)\ , \tag{2.1}$$

where g_Y is the hypercharge gauge coupling and $v \approx 246$ GeV is the electroweak scale. There are no tree-level interactions of the type $B_H H^{(1,0)} h$, $\partial_\mu B_H H^{(1,0)0} Z^\mu$, or $\partial_\mu B_H H^{(1,0)\mp} W^{\mu\pm}$.

The annihilation cross section into a W^+W^- pair (see Fig. 1) is given by

$$\sigma(B_H B_H \to W^+W^-) = \frac{g_Y^4 (s^2 - 4m_W^2 s + 12 m_W^4)}{64\pi s \left(s - m_h^2\right)^2} \left(\frac{s - 4m_W^2}{s - 4M_B^2}\right)^{1/2}\ , \tag{2.2}$$

and the same expression with the W boson mass replaced by the Z boson mass yields the cross section for $B_H B_H$ annihilation into a ZZ pair

$$\sigma(B_H B_H \to ZZ) = \frac{1}{2}\,\sigma(B_H B_H \to W^+W^-)\Big|_{m_W \to m_Z}\ , \tag{2.3}$$

where the factor of 1/2 results from having two identical particles in the final state. Here s is the center-of-mass energy of the collision, while m_W, m_Z and m_h are the the Standard Model masses.

Expanding the cross section in powers of the relative speed between the B_H bosons, v_r, gives

$$v_r\,\sigma\big(B_H B_H \to W^+W^-\big) = a_W + v_r^2 b_W + \mathcal{O}\left(v_r^4\right)\ . \tag{2.4}$$

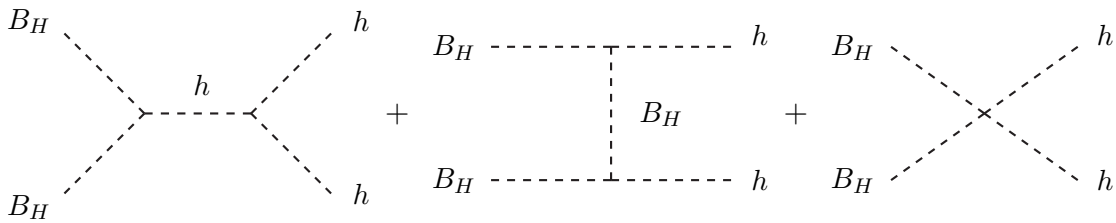

Figure 2: Tree level diagrams for $B_H B_H$ annihilation into hh (the u-channel diagram is not shown).

The first two terms in this non-relativistic expansion are

$$a_W = \frac{2\pi\alpha^2 M_B^2}{c_w^4\left(4M_B^2 - m_h^2\right)^2}\left(1 - \frac{m_W^2}{M_B^2} + \frac{3m_W^4}{4M_B^4}\right)\left(1 - \frac{m_W^2}{M_B^2}\right)^{1/2} \quad , \tag{2.5}$$

and

$$b_W = \frac{-a_W}{4\left(M_B^2 - m_W^2\right)}\left(M_B^2\frac{4M_B^2 + 3m_h^2 - 16m_W^2}{2\left(4M_B^2 - m_h^2\right)} + \frac{3m_W^4\left(2M_B^2 - m_W^2\right)}{4M_B^4 - 4M_B^2 m_W^2 + 3m_W^4}\right) \quad , \tag{2.6}$$

where α is the fine structure constant evaluated at the scale M_B and $c_w = \cos\theta_w$ is the cosine of the weak mixing angle.

The annihilation cross section into a hh pair (see Fig. 2) is given by

$$\sigma(B_H B_H \to hh) = \frac{g_Y^4}{16\pi s}\left[\left(\frac{(s+2m_h^2)^2}{8(s-m_h^2)^2} + \frac{m_Z^4 s_w^4}{m_h^4 + M_B^2(s-4m_h^2)}\right)\left(\frac{s-4m_h^2}{s-4M_B^2}\right)^{1/2}\right.$$
$$\left. + \frac{m_Z^2 s_w^2}{s-4M_B^2}\left(\frac{s+2m_h^2}{s-m_h^2} - \frac{2m_Z^2 s_w^2}{s-2m_h^2}\right)\ln\left(\frac{s-2m_h^2-\sqrt{(s-4M_B^2)(s-4m_h^2)}}{s-2m_h^2+\sqrt{(s-4M_B^2)(s-4m_h^2)}}\right)\right] \quad . \tag{2.7}$$

The corresponding leading terms in the non-relativistic expansion are

$$a_h = \frac{\pi\alpha^2\sqrt{M_B^2 - m_h^2}}{4c_w^4 M_B^3}\left(\frac{2M_B^2 + m_h^2}{4M_B^2 - m_h^2} + \frac{2m_Z^2 s_W^2}{2M_B^2 - m_h^2}\right)^2 \tag{2.8}$$

and

$$b_h = \frac{a_h}{2M_B^2 + m_h^2}\left(-\frac{8M_B^6 + 10M_B^4 m_h^2 - 29M_B^2 m_h^4 + 2m_h^6}{8\left(4M_B^2 - m_h^2\right)\left(M_B^2 - m_h^2\right)}\right.$$
$$\left. + \frac{4}{3}M_B^2 M_Z^2 s_w^2\frac{16M_B^6 - 18M_B^4 m_h^2 + 15M_B^2 m_h^4 - 4m_h^6}{\left(2M_B^2 - m_h^2\right)^2\left[4M_B^4 - m_h^4 - 2M_Z^2 s_w^2\left(4M_B^2 - m_h^2\right)\right]}\right) \quad . \tag{2.9}$$

In the limit in which all the Standard Model particles are much lighter than B_H, the equivalence theorem holds for the boson final states:

$$\sigma_{hh} = \sigma_{ZZ} = \frac{1}{2}\sigma_{W^+W^-} = \frac{g_Y^4}{256\pi M_B^2 v_r}\left(1 - \frac{1}{8}v_r^2 + \cdots\right) \quad . \tag{2.10}$$

2.2 Annihilation into fermion pairs

On general grounds, the interaction between a pair of B_H particles and a pair of fermions is helicity suppressed. To see this note that operators that include a derivative, such as

$$\begin{aligned}\mathcal{O}_1 &= \frac{i}{\Lambda^2} B_H B_H \bar{f}\,\gamma^\mu \partial_\mu f \ , \\ \mathcal{O}_2 &= \frac{1}{\Lambda^2} B_H \left(\partial_\mu B_H\right)\, \bar{f}\gamma^\mu\gamma_5 f \quad ,\end{aligned} \tag{2.11}$$

may be integrated by parts, and then using the Dirac equation take the equivalent form

$$\begin{aligned}\mathcal{O}_1 &= \frac{m_f}{\Lambda^2} B_H B_H\, \bar{f} f \quad , \\ \mathcal{O}_2 &= -\frac{i m_f}{\Lambda^2} B_H B_H\, \bar{f}\gamma_5 f \ .\end{aligned} \tag{2.12}$$

Thus, the two above operators, suppressed by the ratio of the fermion mass m_f to some cutoff scale Λ, are the only independent Lorentz-invariant operators that describe the interactions of two B_H's with a fermion-antifermion pair. These operators are written in an effective theory below the electroweak scale. However, the same arguments apply when the operators are written in an $SU(2)_W \times U(1)_Y$-invariant way, with m_f replaced by $\lambda_f H$ where λ_f is the Yukawa coupling of the fermion to the standard model Higgs doublet H.

The two operators shown in Eq. (2.12) govern the annihilation of spinless photon dark matter to fermions as well as its elastic scattering with nucleons. Hence both these processes will be suppressed by standard model fermion masses. In the 6DSM there are contributions to the operators in Eq. 2.12 from Higgs exchange and (1,0) quark exchange. Higgs exchange contributes only to $\mathcal{O}_1$, whereas KK quark exchange can contribute to both operators. Therefore, the cutoff scale Λ is given in practice by either the mass of a KK quark or by the Higgs boson mass. We will verify these statements by explicit computation of cross sections below, focusing on annihilation to top quarks.

The interaction between the B_H and top quarks takes the following form:

$$\mathcal{L}_t = i\frac{g_Y}{2} B_H \left(y_L\, \bar{T}^{(1,0)}_{+_R} t_L + y_R\, \bar{T}^{(1,0)}_{-_L} t_R \right) + \text{H.c.}\,, \tag{2.13}$$

where $y_L = 1/3$ and $y_R = 4/3$ are the hypercharges of left-handed and right-handed top quark and $P_{L/R} = (1 \mp \gamma_5)/2$ is the projection operator. Interactions with the Standard Model Higgs boson generates off-diagonal elements in the mass matrix of the level-1 top quarks after electroweak symmetry breaking,

$$\begin{pmatrix} \bar{T}^{(1,0)}_- & \bar{T}^{(1,0)}_+ \end{pmatrix} \begin{pmatrix} -\frac{1}{R}\left(1+\Delta_-\right) & m_t(1+\delta_1) \\ m_t(1+\delta_2) & \frac{1}{R}\left(1+\Delta_+\right) \end{pmatrix} \begin{pmatrix} T^{(1,0)}_- \\ T^{(1,0)}_+ \end{pmatrix} , \tag{2.14}$$

where the δs and Δs are radiative corrections to the heavy quark masses. The dominant contribution to these comes from the strong interaction and in the limit that we ignore

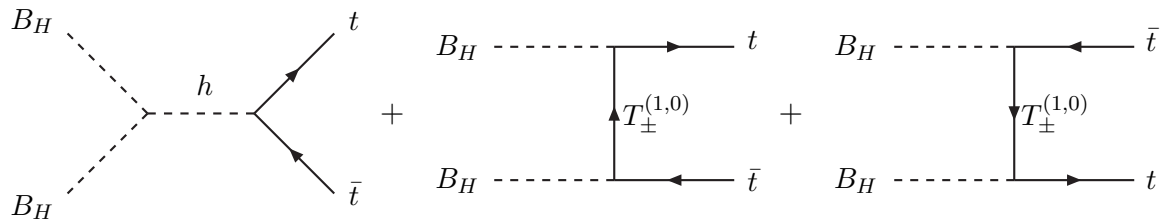

Figure 3: Tree-level diagrams for $B_H B_H$ annihilation into $t\bar{t}$.

electroweak corrections, $\Delta_+ = \Delta_- = \Delta$ and $\delta_1 = \delta_2 = \delta$. The diagonal correction Δ was computed in Ref. [20] to be equal to

$$\Delta = \frac{16}{3}\frac{g_s^2}{8\pi^2}\log(\Lambda R) + \frac{m_t^2 R^2}{2} + \mathcal{O}\left(\frac{g^2}{g_s^2}, \frac{g_Y^2}{g_s^2}, \frac{\lambda_t^2}{g_s^2}\right) , \tag{2.15}$$

where g_Y, g and g_s are the $SU(3)_c \times SU(2)_W \times U(1)_Y$ gauge couplings, λ_t is the top Yukawa coupling, m_t is the Standard Model top quark mass, and Λ is the cut-off scale. We take $\Lambda \approx 10/R$ based on naive dimensional analysis [17]. Although δ has not been computed, it is expected to be of the same order as Δ, and we will take these to be equal for the remainder of this paper.

The weak eigenstates are related to mass eigenstates by

$$\begin{pmatrix} T_-^{(1,0)} \\ T_+^{(1,0)} \end{pmatrix} = \begin{pmatrix} -\gamma_5 c_\alpha & s_\alpha \\ \gamma_5 s_\alpha & c_\alpha \end{pmatrix} \begin{pmatrix} T'^{(1,0)}_- \\ T'^{(1,0)}_+ \end{pmatrix} , \tag{2.16}$$

where $c_\alpha = \cos\alpha$, $s_\alpha = \sin\alpha$ for a mixing angle α given by $\tan 2\alpha = m_t R$. The mass eigenstates, $T'^{(1,0)}_-$ and $T'^{(1,0)}_+$ have the same mass

$$M_T = \sqrt{\frac{1}{R^2} + m_t^2}(1+\Delta) . \tag{2.17}$$

In the mass eigenstate basis the B_H-top quark interaction can be written as

$$\mathcal{L}_t = i\frac{g_Y}{2} B_H \left[\bar{T}'^{(1,0)}_- \left(y_L P_L s_\alpha + y_R P_R c_\alpha\right) t + \bar{T}'^{(1,0)}_+ \left(y_L P_L c_\alpha + y_R P_R s_\alpha\right) t\right] + \text{H.c.} . \tag{2.18}$$

Since we will only deal with the quark mass eigenstates, we will omit all primes in what follows.

The relativistic annihilation cross section into top quarks, computed at tree level, is given by

$$\sigma\left(B_H B_H \to t\bar{t}\right) = \frac{3 g_Y^4}{8\pi s\left(s - 4M_B^2\right)} \int_{t_-}^{t_+} dt \left[-\frac{y_L^4 + y_R^4}{16} B(t) + \frac{y_L y_R}{8} m_t^2 A_T(t) + m_t^2 A_h(t)\right] , \tag{2.19}$$

where the terms collected in $B(t)$ are due to exchange of the gauge eigenstates of the T quark, without interference terms,

$$B(t) = \frac{t^2 + t\left(s - 2M_B^2\right) + \left(M_H^2 - m_t^2\right)^2}{\left(t - M_T^2\right)^2} + \frac{t^2 + t\left(s - 2M_B^2 - 2m_t^2\right) + M_B^4 - m_t^4}{\left(M_T^2 - M_B^2 - m_t^2 + s/2\right)\left(t - M_T^2\right)} \ . \tag{2.20}$$

The contributions from an electroweak mass insertion on the T quark line are included in

$$A_T(t) = \frac{-1}{\left(t - M_T^2\right)^2}\left\{y_L y_R\left[2t - (1+\delta)^2\left(s - 4m_t^2\right)\right] + 2\left(y_L^2 + y_R^2\right)(1+\delta)\left(t - M_B^2 + m_t^2\right)\right\}$$

$$- \frac{y_L y_R\left[2\left(M_B^2 - m_t^2\right) + (1+\delta)^2\left(s - 4m_t^2\right)\right] + \left(y_L^2 + y_R^2\right)(1+\delta)\left(s - 4m_t^2\right)}{\left(M_T^2 - M_B^2 - m_t^2 + s/2\right)\left(t - M_T^2\right)} \ . \tag{2.21}$$

Finally, $A_h(t)$ includes the contributions due to Higgs boson exchange,

$$A_h(t) = \frac{-\left(y_L^2 + y_R^2\right)\left(t - M_B^2 + m_t^2\right) + y_L y_R(1+\delta)\left(s - 4m_t^2\right)}{2\left(s - m_h^2\right)\left(t - M_T^2\right)} + \frac{s - 4m_t^2}{4\left(s - m_h^2\right)^2} \ . \tag{2.22}$$

The integration limits of the Mandelstam variable, t, are given by

$$t_{\mp} = M_B^2 + m_t^2 - \frac{s}{2} \mp \frac{1}{2}\sqrt{\left(s - 4M_B^2\right)\left(s - 4m_t^2\right)} \ . \tag{2.23}$$

After integrating over t in Eq. (2.19), we find the following leading terms in the non-relativistic expansion for σv_r

$$a_t = \frac{3\pi\alpha^2}{4c_w^4}\frac{m_t^2}{M_B^3}\left(M_B^2 - m_t^2\right)^{3/2}\left(\frac{(y_L + y_R)^2 + 2y_L y_R\delta}{M_T^2 + M_B^2 - m_t^2} - \frac{2}{4M_B^2 - m_h^2}\right)^2 \ , \tag{2.24}$$

and

$$b_t = -\frac{a_t}{24}\left[6 - \frac{M_B^2}{M_B^2 - m_t^2}\left(1 - \frac{4M_T^2}{M_T^2 + M_B^2 - m_t^2}\right)^2 + \frac{8M_B^2}{4M_B^2 - m_h^2}\right. \tag{2.25}$$

$$\left. \times \frac{\left(y_L^2 + y_R^2\right)\left(4M_B^2 - m_h^2\right)^2 + 2\left(3M_T^2 + M_B^2 - m_t^2\right)\left(4M_B^2 - m_h^2\right) - 12\left(M_T^2 + M_B^2 - m_t^2\right)^2}{\left[(y_L + y_R)^2 + 2y_L y_R\delta\right]\left(M_T^2 + M_B^2 - m_t^2\right)\left(4M_B^2 - m_h^2\right) - 2\left(M_T^2 + M_B^2 - m_t^2\right)^2}\right] .$$

This computation confirms that annihilation into $t\bar{t}$ is suppressed by m_t^2/M_B^2 due to helicity flipping. Note the relative minus sign in Eq. 2.24 between the Higgs-exchange and heavy top exchange contibutions. This interference leads to further suppression of this annihilation channel.

3. Relic abundance

We begin this section with a review of the standard calculation for the thermal relic abundance of a stable, massive particle [22]. We then compute the relic abundance for the spinless photon in order to determine the range of M_B, the spinless photon mass, consistent with the observed abundance of dark matter.

3.1 From annihilation cross sections to relic abundance

The relic abundance of B_H is given by solving Boltzmann's equation for the evolution of its number density, n,

$$\frac{dn}{dt} = -3Hn - \langle \sigma v_r \rangle \left(n^2 - n_{\rm eq}^2 \right) \ , \tag{3.1}$$

where H is the Hubble parameter, $\langle \sigma v_r \rangle$ is the thermal average of the total annihilation cross section of B_H times the relative velocity of the annihilating particles, and $n_{\rm eq}$ is their equilibrium number density.

An approximate analytical solution can be found for early and late times. At temperatures substantially above the spinless photon mass ($T \gg M_B$) there are roughly as many B_H particles as photons and $n_{\rm eq} \sim T^3$. For temperatures below M_B the equilibrium density is Boltzmann-suppressed and is given in the non-relativistic approximation by

$$n_{\rm eq} = \left(\frac{M_B\, T}{2\pi} \right)^{3/2} e^{-M_B/T} \ . \tag{3.2}$$

As the temperature decreases still further the B_H annihilation rate eventually drops below the Hubble expansion rate so B_H cannot remain in equilibrium and becomes a thermal relic. From this point on, the total number of B_H particles stays constant, with a number density diluted by the expansion of the universe. The temperature at which this takes place is known as the freeze-out temperature, T_F, and is roughly determined by equating the dark matter annihilation rate to the expansion rate of the universe

$$\langle \sigma v_r \rangle n|_{T=T_F} \sim H \ , \tag{3.3}$$

giving the following equation which can be solved iteratively for T_F:

$$\frac{M_B}{T_F} = \ln \left[c(c+2) \frac{3}{4\pi^3} \left(\frac{5 M_B\, T_F}{2 g_*} \right)^{1/2} M_{\rm Pl} \langle \sigma v_r \rangle \Big|_{T=T_F} \right] \ . \tag{3.4}$$

Here, $M_{\rm Pl} = 1.22 \times 10^{19}$ GeV is the Planck scale, g_* is the total number of effectively massless degrees of freedom at the freeze-out temperature and c is an $O(1)$ constant that is determined by comparing to numerical solutions of the Boltzmann equation. Note that because of its logarithmic dependence on mass and cross section, the ratio of the freeze-out temperature to the dark matter mass is relatively insensitive to these quantities.

In the non-relativistic limit the thermally averaged annihilation cross section can be expressed as

$$\langle \sigma v_r \rangle = a + 6\, b\, \frac{T_F}{M_B} + \cdots \ , \tag{3.5}$$

where the a- and b-terms are sums over the contributions for W^+W^-, ZZ, hh and $t\bar{t}$ final states given in Eqs. (2.5)-(2.9), (2.24) and (2.26). Using this approximation one can match the early and late-time solutions to the Boltzmann equation to find the current B_H density,

$$\Omega_{B_H} h^2 \approx \frac{1.04 \times 10^9 \ {\rm GeV}^{-1}}{M_{\rm Pl} \sqrt{g_*}} \frac{M_B/T_F}{a + 3\, b\, T_F/M_B} \ , \tag{3.6}$$

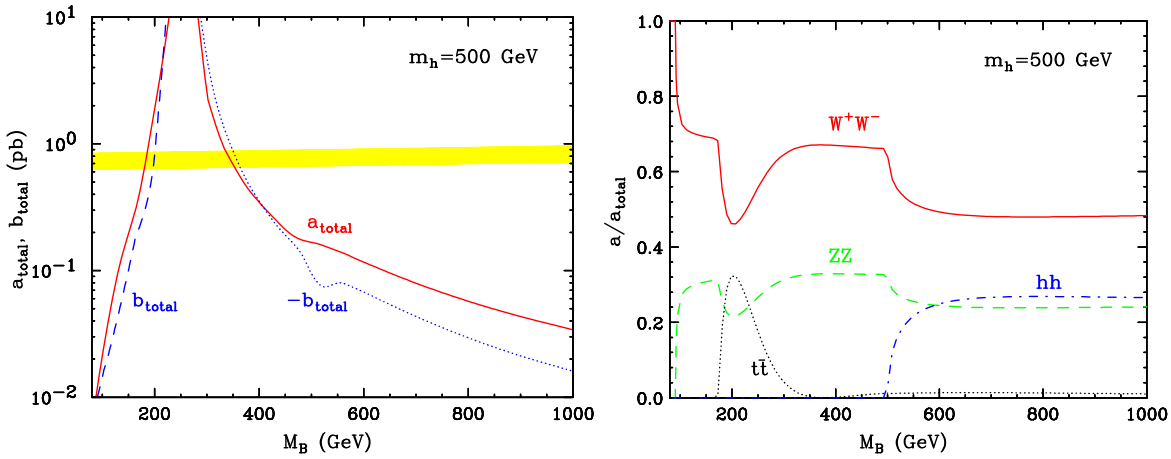

Figure 4: Left: The coefficients a and b from the non-relativistic expansion of the total B_H annihilation cross section. The shaded band corresponds to the current range of a measured by WMAP ($0.096 < \Omega_{B_H} h^2 < 0.122$ at 2σ) and b includes the relativistic correction, $-a/4$. Right: the relative contribution to $a_{\rm total}$ from various final states. Note that the non-relativistic expansion fails near the Higgs s-channel resonance, $2M_B = m_h = 500$ GeV.

where the dimensionful constant in the numerator comes from factors of the current critical density and entropy density. A more careful treatment of this method [22] results in additional sub-leading terms which can be accounted for by the replacement $b \to b - a/4$ in the above formulas.

Note that the non-relativistic expansion fails near s-channel resonances and final state thresholds [23] and the relic abundance in the vicinity of these must be calculated by alternative methods. A treatment of resonances in models with one universal extra dimension can be found in Ref. [7].

3.2 Prediction for the spinless photon mass

For the remainder of this analysis we will ignore Δ, the one-loop QCD correction to quark masses, since this quantity has a negligible effect on our results. Furthermore, since we have no robust information on the exact value of the Higgs mass, we take this to be a free parameter. For Higgs masses near $2M_B$, there is a resonance effect from an s-channel Higgs going on shell. Away from this resonance and all mass thresholds, the non-relativistic expansion of the annihilation cross section is a valid approximation and the relic abundance can be computed analytically using the expressions for the annihilation cross sections given in Sec. 2.2. These were verified using our implementation [25] of the 6DSM in `CalcHEP` [26].

In the left frame of Fig. 4 we plot the a- and b-term contributions to the total annihilation cross section for a heavy Higgs boson, with the shaded region corresponding to the range consistent with current WMAP data ($0.096 < \Omega_{B_H} h^2 < 0.122$ at 2σ) [24]. In the regions away from the Higgs resonance, the total b-term is smaller than the a-term, although it becomes significant near the resonance due to the higher power of the mass difference $4M_B^2 - m_h^2$ in its

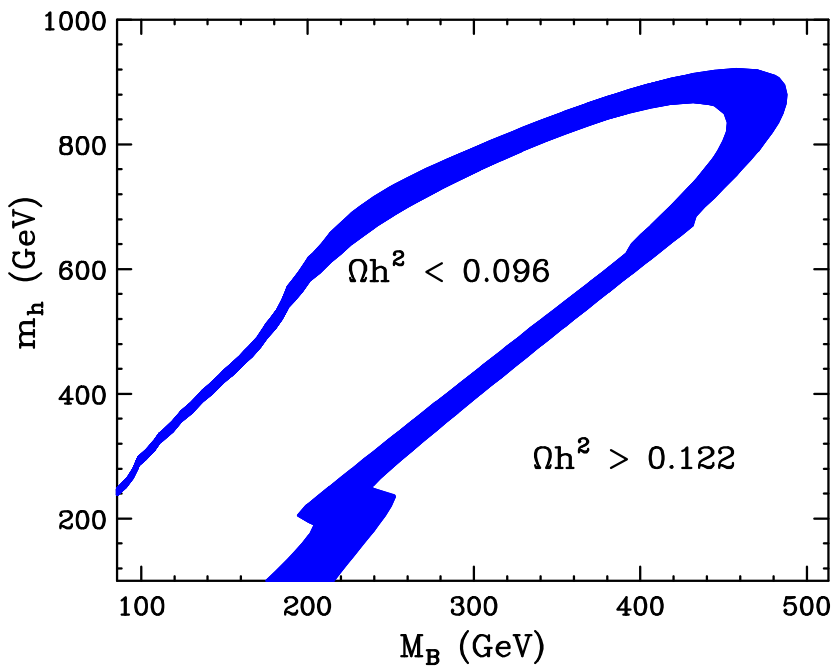

Figure 5: The region (shaded) of the m_h vs. M_B plane in which the B_H thermal relic abundance is within the range measured by WMAP ($0.096 < \Omega_{B_H} h^2 < 0.122$).

denominator, in comparison with the a-term. Even near the resonance, however, the effect of the b-term contribution on the relic abundance is suppressed by the velocity ($v_r^2 \sim 0.1$) and impacts the dark matter density at about the 10% level or less.

As shown in the left frame of Fig. 4, there are two regions consistent with WMAP around the Higgs resonance, $M_B \sim 180$ GeV and $M_B \sim 350$ GeV. Note that in contrast to the 5D case [3, 6] a light range of dark matter masses is preferred by data. This difference is to a large extent due to the spin of the dark matter candidate. The dominant annihilation channel of the spin-1 dark matter candidate in 5D is to fermion pairs, whereas annihilation of spinless photons to pairs of light fermions is helicity suppressed. The multiplicity of light fermion final states allows the former to annihilate more efficiently, leading to an increase in its mass in order to remain consistent with data.

The relative contributions to the total annihilation cross section from different final states are plotted for a large Higgs mass in the right frame of Fig. 4. We see that annihilation to boson final states is dominant for a spinless photon mass above the boson production threshold. As expected from the Goldstone boson equivalence theorem, the a-term for the W^+W^- final state is twice that for the ZZ and hh final states in the limit of large M_B. The top quark final state is only significant for a small range of parameters; it is below threshold for $M_B \lesssim 170$ GeV and helicity suppressed for large values of M_B.

Note that the results in this figure are not reliable in the region of $M_B \approx 250$ GeV as this corresponds to a spinless photon mass that is exactly half the Higgs mass and the

Higgs is on resonance. In such a case we can no longer use the non-relativistic expansion of the annihilation cross-section, and instead calculate the relic abundance numerically using `micrOMEGAs` [27]. Our results are shown in Fig. 5 for different values of m_h and M_B, with the shaded region corresponding to parameters that are consistent with the current WMAP measurements. In this figure we see again two possible regions of M_B for each value of the Higgs mass, with the region at smaller M_B containing a significant contribution from annihilation to top pairs, this final state being helicity suppressed in the other region. For instance, for a Higgs mass of 500 GeV, the light B_H region ($M_B \sim 180$ GeV) has less than 20% contribution from annihilation to $t\bar{t}$, with the remainder shared between W^+W^- and ZZ in accordance with the equivalence theorem; whereas for a heavy B_H ($M_B \sim 350$ GeV) there is a negligible contribution from $t\bar{t}$. These relative contributions from different final states can be read directly from Fig. 4.

We expect effects of coannihilation with other level-1 states to be small due to larger mass splittings between the modes as compared with those in 5D [3, 6], and we do not include these in our analysis. Our results are relatively insensitive to exotic Higgs decays since their contributions to the total width of the Higgs are small. Moreover, they are also mostly independent of the rest of the KK spectrum of the 6DSM. Recall that only annihilation to top quarks involves any additional heavy modes, and that this contribution is subdominant over most of the parameter space.

4. Astrophysical Detection

Efforts to detect dark matter particles with astrophysical experiments are often classified as direct or indirect detection. Direct detection experiments are those which attempt to observe particles scattering elastically with the detector, whereas indirect detection efforts attempt to observe the dark matter annihilation products [28].

4.1 Direct Detection

In this section, we discuss the prospect for the direct detection of spinless photon dark matter. A spinless photon can scatter elastically with a quark through the exchange of a KK-quark or a Higgs boson (see Fig. 6). The leading term in the amplitude due to Higgs exchange is given in the non-relativistic limit by

$$\mathcal{M}_h = i\,\frac{g_Y^2}{2}\frac{m_q}{m_h^2}\,\bar{q}q\,, \tag{4.1}$$

where q is a quark field of mass m_q. Similarly the amplitude for KK quark exchange is given by

$$\begin{aligned}\mathcal{M}_Q = -i\frac{g_Y^2}{4}\Big[&(y_L^2+y_R^2)\Big(\frac{m_q-M_B}{(m_q-M_B)^2-M_Q^2}+\frac{m_q+M_B}{(m_q+M_B)^2-M_Q^2}\Big)\bar{q}\,\gamma^0\,q\\ &+2M_Q y_L y_R \sin 2\alpha\Big(\frac{1}{(m_q-M_B)^2-M_Q^2}+\frac{1}{(m_q+M_B)^2-M_Q^2}\Big)\bar{q}q\Big]\,.\end{aligned} \tag{4.2}$$

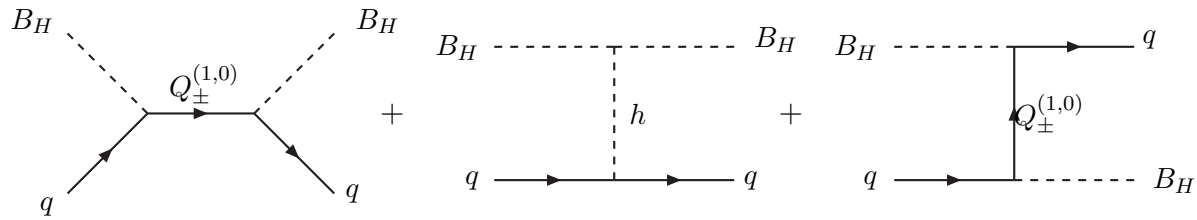

Figure 6: Tree-level diagrams for the elastic scattering of the B_H with quarks.

Summing $\mathcal{M}_h$ and $\mathcal{M}_Q$, we obtain

$$\langle \mathcal{M} \rangle = \mathcal{C}_q \langle \bar{q} q \rangle \,, \tag{4.3}$$

where we have combined terms using $\bar{q}\gamma^0 q \approx \bar{q}q$ and $\bar{q}\gamma^5 q \approx 0$ which hold in the non-relativistic limit. $\langle\ \rangle$ denotes an average and sum over the spins of the initial and final state quarks respectively. The coefficient $\mathcal{C}_q$ may be read directly from the matrix elements (4.1) and (4.2),

$$\begin{aligned}\mathcal{C}_q = \frac{g_Y^2}{4} \Bigg[& m_q (y_L + y_R)^2 \left(\frac{1}{M_Q^2 - (m_q - M_B)^2} + \frac{1}{M_Q^2 - (m_q + M_B)^2} \right) \\ & + M_B (y_L^2 + y_R^2) \left(\frac{1}{M_Q^2 - (m_q + M_B)^2} - \frac{1}{M_Q^2 - (m_q - M_B)^2} \right) + \frac{2 m_q}{m_h^2} \Bigg] \,. \end{aligned} \tag{4.4}$$

The propagators in this expression can be expanded to linear order in m_q to obtain

$$\mathcal{C}_q \approx \frac{g_Y^2}{2} m_q \left(\frac{1}{m_h^2} + \frac{(y_L + y_R)^2}{M_Q^2 - M_B^2} + \frac{2\left(y_L^2 + y_R^2\right) M_B^2}{\left(M_Q^2 - M_B^2\right)^2} \right) \,. \tag{4.5}$$

The expression in Eq. (4.4) diverges for $M_Q = |M_B \pm m_q|$. Given that we are ultimately interested in elastic scattering off nucleons, the top quark contributes only at one loop through the effective coupling of a pair of B_Hs to two gluons. For simplicity, we treat the contribution from the top quark in the same way as that from the b or c quarks. The validity of this procedure would need to be checked by a full loop calculation of B_H-gluon elastic scattering, which would allow one to assess whether there are any resonance effects.

Note that effects from electroweak mass mixing that flip the chirality of the (1,0) quarks (proportional to $y_L y_R$ in the above equation) are of the same order as the pieces that flip the chirality of the external quark lines, and may not be neglected.[1] As anticipated from the discussion in Sec. 2.2 of higher-dimension operators contributing to the elastic scattering process, the entire B_H-quark elastic scattering cross section is proportional to m_q.

[1] In the 5D case, we expect that similar terms, which have been omitted so far in the literature, will increase the contribution from KK quark exchange to the elastic scattering cross section.

The matrix element $\langle \bar{q}q \rangle$ of quarks in a nucleon state can be evaluated [29] to obtain

$$\langle \bar{q}q \rangle = \frac{m_{p,n}}{m_q} f_{T_q}^{p,n} \text{ (light quarks) ; } \langle \bar{q}q \rangle = \frac{2}{27} \frac{m_{p,n}}{m_q} f_{TG}^{p,n} \text{ (heavy quarks) .} \tag{4.6}$$

Summing over quark flavors, we arrive at the B_H-nucleon couplings:

$$f_{p,n}^{B_H} = m_{p,n} \sum_{q=u,d,s} \frac{\mathcal{C}_q}{m_q} f_{T_q}^{p,n} + \frac{2m_{p,n}}{27} f_{TG}^{p,n} \sum_{q=c,b,t} \frac{\mathcal{C}_q}{m_q} , \tag{4.7}$$

where the quantities $f_{T_q}^{p,n}$ have been measured to be $f_{T_u}^p = 0.020 \pm 0.004$, $f_{T_d}^p = 0.026 \pm 0.005$, $f_{T_s}^p = 0.118 \pm 0.062$, $f_{T_u}^n = 0.014 \pm 0.003$, $f_{T_d}^n = 0.036 \pm 0.008$ and $f_{T_s}^n = 0.118 \pm 0.062$ [30]. The first term in this expression corresponds to interactions with quarks in the target nucleon, whereas the second term results from interactions with gluons through a quark or heavy quark loop. f_{TG}^p is given by $1 - f_{T_u}^p - f_{T_d}^p - f_{T_s}^p \approx 0.84$ and analogously, $f_{TG}^n \approx 0.83$.

The total B_H-nucleus cross section at zero momentum transfer is given by

$$\sigma = \frac{m_N^2}{4\pi(M_B + m_N)^2} \left(Z f_p^{B_H} + (A - Z) f_n^{B_H} \right)^2 , \tag{4.8}$$

where m_N, Z and A are the mass, atomic number and atomic mass of the target nuclei. Although the experimental sensitivities and limits are often described in terms of the dark matter elastic scattering with nucleons, one should keep in mind that the nuclear form factors may need to be taken into account.

Note that there is no spin-dependent contribution to the elastic scattering cross section. This is in contrast with the 5D case, where the spin-dependent $B_\mu^{(1)}$-nucleus elastic scattering cross section is typically three or four orders of magnitude larger than the corresponding spin-independent cross section [4, 8], and only the average over the nucleons inside the nucleus suppresses the spin-dependent effects.

In Fig. 7 we compare the spin-independent elastic scattering cross section of the B_H to the current and projected sensitivities of direct detection experiments. At present, the strongest limits have been placed by the XENON [31] and CDMS [32] collaborations. These constraints are, however, not yet sensitive to the range of cross sections predicted in this model. Only with future experimental programs, such as the first phase of Super-CDMS or a 100 kilogram version of LUX, will direct detection experiments begin to reach the sensitivity needed to test this model. To test the region with M_B of order several hundred GeV and larger, the full phase-C of super-CDMS or a multi-ton liquid noble detector will likely be required [33].

4.2 Indirect detection

Efforts to detect the annihilation products of dark matter particles in the form of gamma rays, antimatter and neutrinos are collectively known as indirect detection. In this section, we discuss the prospects for the indirect detection of spinless photon dark matter.

Dark matter particles annihilating in the galactic halo or in dark matter substructures may potentially generate observable fluxes of annihilation products in the form of gamma

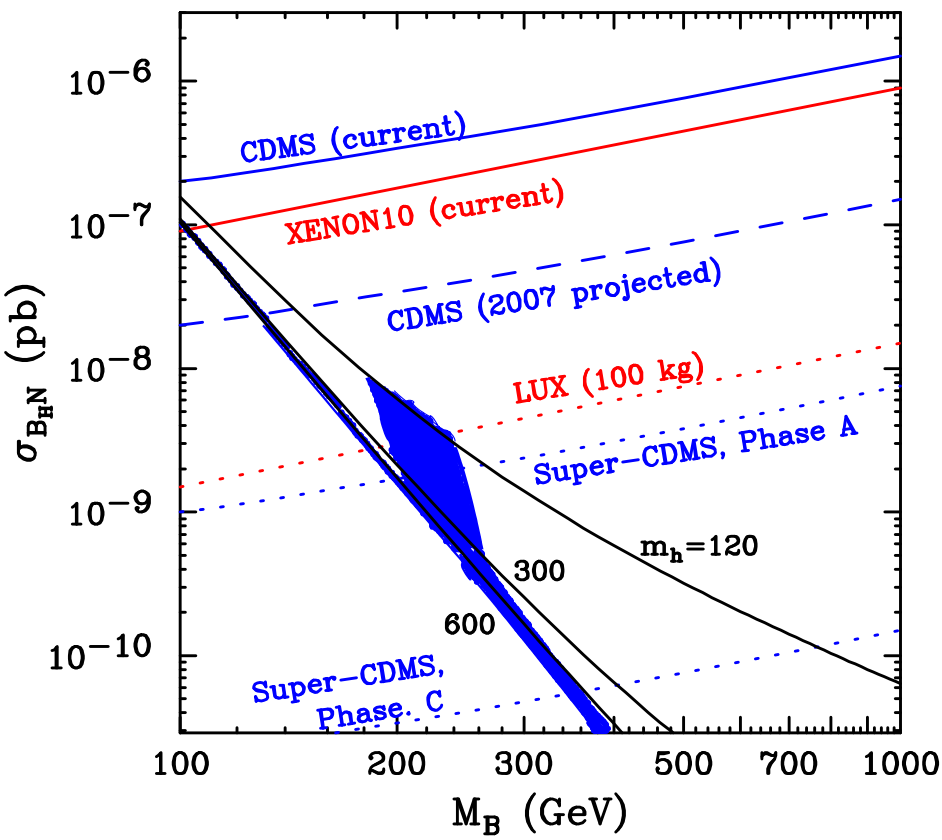

Figure 7: Prospects for the direct detection of B_H dark matter. Predicted cross sections are shown as black solid lines for Higgs masses of 120, 300 and 600 GeV. Current constraints are shown as blue (CDMS) and red (XENON) solid lines. The dashed blue line denotes the near term projection from the CDMS experiment. The dotted lines represent longer term projections. Shown as a filled blue region is the parameter range in which the observed abundance of dark matter can be generated in this model.

rays, positrons, anti-protons or anti-deuterons. The prospects for searches of such particles depend strongly on unknown astrophysical inputs, such as the distribution of dark matter and the structure of galactic magnetic fields. The only particle physics inputs which are relevant to gamma ray and antimatter searches for dark matter are particle's mass, annihilation cross section in the low velocity limit and the species of Standard Model particles that are generated in those annihilations.

The low velocity cross section for spinless photon annihilations is dictated by the relic abundance calculation to be $\sigma v \approx 3 \times 10^{-26}$ cm^3/s $\approx$1 pb. These annihilations largely result in the production of gauge and Higgs boson pairs. This is very similar to the characteristics found for a wino-like or higgsino-like neutralino, leading to very similar prospects and signatures in gamma ray and antimatter based dark matter searches. Instead of repeating the phenomenology of these indirect detection channels here, we refer the reader to previous studies on the subjects of dark matter searches with gamma rays [34] and antimatter [35]. We

will, however, mention briefly the differences found between the 6D and 5D cases regarding these.

In the case of 5D, the $B_\mu^{(1)}$ annihilations generate mostly charged lepton pairs (approximately 20% to each family). In addition to the standard gamma ray spectrum from cascade decays and fragmentation, the electron-positron pairs produce a harder gamma ray spectrum via final state radiation. The tau pairs produced also generate a harder spectrum through their decays [13]. In 6D, the annihilations to gauge and Higgs bosons do not result in such a hard spectrum.

In addition, annihilations to electron-positron pairs in and other charged leptons in 5D result in a particularly hard spectrum of positrons in the cosmic ray spectrum [4, 12]. The contribution from annihilations to W^+W^- in the 6DSM is also somewhat hard, but much less so than is found in the 5D case. As with the gamma ray spectrum, the positron spectrum resulting from dark matter annihilations in this model more closely resembles the signal predicted from neutralino annihilations than from the case of 5D models.

Dark matter particles which undergo elastic scattering with nuclei in the Sun or Earth can become gravitationally bound to these bodies, and accumulate in their cores. Once captured in sufficient numbers, they can annihilate efficiently, producing a sizable flux of energetic Standard Model particles. Of these annihilation products, only neutrinos can escape from the Sun or Earth and potentially be observed [36].

The capture rate of dark matter particles depends on their elastic scattering cross section with nuclei. Unfortunately, this cross section is rather small in the model considered here. Over the entire range of parameters considered here, the elastic scattering cross section is never larger than $\sim 10^{-7}$ pb, which leads to less than one neutrino being observed from dark matter annihilations in the Sun per ten years in a kilometer-scale experiment [37]. The rate from the Earth is even smaller. This is very different from the neutrino rate predicted in the 5D case. The reason for this distinction is that spin-dependent scattering is significant in 5D, leading to typical rates of $\sim 0.1 - 100$ per square kilometer per year [10].

5. Conclusions

Despite the experimental successes of the Standard Model, it does not contain a viable candidate for dark matter. This absence is one of the strongest motivations for the existence of physics beyond the Standard Model. In particular, dark matter is a primary motivation for supersymmetry since models with R-parity conservation can provide a viable dark matter candidate. Recently, there has been greater attention placed on other types of dark matter candidates, including those found in models with universal extra dimensions, where the stability of dark matter is due to a discrete symmetry called KK parity. In the minimal model with one universal extra dimension, dark matter typically consists of a KK excitation of the hypercharge gauge boson. This 5D KK dark matter has strikingly different phenomenology from neutralinos in supersymmetric models [38]. Models with one universal extra dimension may also contain other viable dark matter candidates, including the KK modes of the graviton

[14] and right-handed neutrinos [16]. Certain models with two universal extra dimensions, where the dark matter particle is a KK mode of the hypercharge vector boson or right-handed neutrinos, have also been investigated [3, 39].

In this paper we have studied the possibility of KK dark matter in the 6DSM [20], which is the minimal model with two universal extra dimensions. The lightest KK-parity odd state is a spin-0 excitation of the hypercharge boson, B_H, referred to as the spinless photon. We have computed annihilation cross sections necessary for the calculation of relic density in this model, and found the regions of parameter space in which the measured abundance of dark matter is generated.

Unlike KK dark matter in the 5D case, B_H annihilations into fermion final states is helicity suppressed because B_H has spin 0. Thus, all fermion final states other than top quarks are negligible, and final states with bosons are dominant. In order for the B_H to sufficiently annihilate and to generate the desired thermal relic density its mass must satisfy $M_B \lesssim 500$ GeV. In the 6DSM this corresponds to a compactification scale of $1/R \lesssim 600$ GeV, which is considerably smaller than the range favored in the 5D case.

It is tempting to compare this upper limit with the lower limit from searches at the Tevatron, of almost 300 GeV [21]. However, one should keep in mind that perturbations of the mass spectrum due to localized operators could change the limit from relic abundance independently of the collider limits, as they depend on different (1,0) masses. The limits from electroweak observables have not been computed in the 6DSM, and are likely in any case to be sensitive to contributions from the unknown physics at the cutoff scale.

We have also studied the prospects for observing B_H dark matter in direct and indirect dark matter experiments. We find that the elastic scattering cross section of this particle with nuclei is completely spin-independent, and is smaller than the current sensitivity of direct detection experiments. Only the next-generation experiments will start probing significant regions of the parameter space. Moreover this small spin-independent cross section results in a prediction of very small rates at neutrino telescopes. The phenomenology of the spinless photon in the context of astrophysical detection resembles neutralino dark matter in many respects, and is distinctively different from KK dark matter in models with one universal extra dimension.[2]

These conclusions could potentially be modified once other effects are considered. In particular, a pair of B_H's may annihilate via an s-channel (2,0) Higgs exchange, and if the masses are near the resonance that could be a large effect even though the coupling of the (2,0) modes to standard model particles are suppressed (a similar situation occurs in the case of one universal extra dimension [7]). Furthermore, the mixing of B_H with the spinless Z-boson, the next lightest KK mode, may be an important effect for small M_B. In this scenario we expect to see a non-negligible increase of the B_H mass in order for the relic abundance to remain consistent with WMAP measurements. Coannihilations tend to increase the range

[2]The collider phenomenology of the 6DSM, on the other hand, is quite different from either supersymmetry or one universal extra dimension. It includes distinctive multi-lepton plus photon signatures [21], and multiple $t\bar{t}$ resonances [17].

of dark matter masses which yield the measured abundance of dark matter regardless of the Higgs mass [6]. Higher-order corrections to the annihilation cross section are known to be non-negligible, especially in the case of coannihilation with colored particles and when quarks are in the final state. In our study, however, this only applies to annihilation to $t\bar{t}$, which is somewhat suppressed compared to annihilation to W^+W^-, ZZ and hh.

Dark matter candidates other than the spinless photon may be possible in the 6DSM if the (1,0) spectrum is modified by localized operators. These include the (1,0) modes of the graviton, right-handed neutrino, Higgs boson, or electroweak bosons. We leave a further exploration of these possibilities to future studies.

Acknowledgments: Many thanks to Jonathan Feng, Geraldine Servant and especially to Tim Tait for useful comments. Fermilab is operated by Fermi Research Alliance, LLC under Contract No. DE-AC02-07CH11359 with the United States Department of Energy. DH is also supported by NASA grant NAG5-10842.

References

[1] T. Appelquist, H. C. Cheng and B. A. Dobrescu, "Bounds on universal extra dimensions," Phys. Rev. D **64**, 035002 (2001) [arXiv:hep-ph/0012100].

[2] H. C. Cheng, K. T. Matchev and M. Schmaltz, "Radiative corrections to Kaluza-Klein masses," Phys. Rev. D **66**, 036005 (2002) [arXiv:hep-ph/0204342].

[3] G. Servant and T. M. Tait, "Is the lightest Kaluza-Klein particle a viable dark matter candidate?," Nucl. Phys. B **650**, 391 (2003) [arXiv:hep-ph/0206071].

[4] H. C. Cheng, J. L. Feng and K. T. Matchev, "Kaluza-Klein dark matter," Phys. Rev. Lett. **89**, 211301 (2002) [arXiv:hep-ph/0207125].

[5] For a recent review, see D. Hooper and S. Profumo, "Dark matter and collider phenomenology of universal extra dimensions," Phys. Rept., in press, arXiv:hep-ph/0701197.

[6] K. Kong and K. T. Matchev, "Precise calculation of the relic density of Kaluza-Klein dark matter in universal extra dimensions," JHEP **0601**, 038 (2006) [arXiv:hep-ph/0509119]; F. Burnell and G. D. Kribs, "The abundance of Kaluza-Klein dark matter with coannihilation," Phys. Rev. D **73**, 015001 (2006) [arXiv:hep-ph/0509118].

[7] M. Kakizaki, S. Matsumoto, Y. Sato and M. Senami, "Significant effects of second KK particles on LKP dark matter physics," Phys. Rev. D **71**, 123522 (2005) [arXiv:hep-ph/0502059]; "Relic abundance of LKP dark matter in UED model including effects of second KK resonances," Nucl. Phys. B **735**, 84 (2006) [arXiv:hep-ph/0508283]; M. Kakizaki, S. Matsumoto and M. Senami, "Relic abundance of dark matter in the minimal universal extra dimension model," Phys. Rev. D **74**, 023504 (2006) [arXiv:hep-ph/0605280].

[8] G. Servant and T. M. P. Tait, "Elastic scattering and direct detection of Kaluza-Klein dark matter," New J. Phys. **4**, 99 (2002) [arXiv:hep-ph/0209262].

[9] D. Majumdar, "Detection rates for Kaluza-Klein dark matter," Phys. Rev. D **67**, 095010 (2003) [arXiv:hep-ph/0209277].

[10] D. Hooper and G. D. Kribs, "Probing Kaluza-Klein dark matter with neutrino telescopes," Phys. Rev. D **67**, 055003 (2003) [arXiv:hep-ph/0208261].

[11] G. Bertone, G. Servant and G. Sigl, "Indirect detection of Kaluza-Klein dark matter," Phys. Rev. D **68**, 044008 (2003) [arXiv:hep-ph/0211342];
T. Bringmann, "High-energetic cosmic antiprotons from Kaluza-Klein dark matter," JCAP **0508**, 006 (2005) [arXiv:astro-ph/0506219];
A. Barrau, *et al*, "Kaluza-Klein dark matter and galactic antiprotons," Phys. Rev. D **72**, 063507 (2005) [arXiv:astro-ph/0506389];

[12] D. Hooper and G. D. Kribs, "Kaluza-Klein dark matter and the positron excess," Phys. Rev. D **70**, 115004 (2004) [arXiv:hep-ph/0406026].

[13] L. Bergstrom, T. Bringmann, M. Eriksson and M. Gustafsson, "Gamma rays from Kaluza-Klein dark matter," Phys. Rev. Lett. **94**, 131301 (2005) [arXiv:astro-ph/0410359]; "Two photon annihilation of Kaluza-Klein dark matter," JCAP **0504**, 004 (2005) [arXiv:hep-ph/0412001].

[14] J. L. Feng, A. Rajaraman and F. Takayama, "Superweakly-interacting massive particles," Phys. Rev. Lett. **91**, 011302 (2003) [arXiv:hep-ph/0302215]; "Graviton cosmology in universal extra dimensions," Phys. Rev. D **68**, 085018 (2003) [arXiv:hep-ph/0307375];
N. R. Shah and C. E. M. Wagner, "Gravitons and dark matter in universal extra dimensions," Phys. Rev. D **74**, 104008 (2006) [arXiv:hep-ph/0608140].

[15] J. A. R. Cembranos, J. L. Feng and L. E. Strigari, "Exotic collider signals from the complete phase diagram of minimal universal extra dimensions," Phys. Rev. D **75**, 036004 (2007) [arXiv:hep-ph/0612157].

[16] S. Matsumoto, J. Sato, M. Senami and M. Yamanaka, "Solving cosmological problem in universal extra dimension models by introducing Dirac neutrino," Phys. Lett. B **647**, 466 (2007) [arXiv:hep-ph/0607331]; "Relic abundance of dark matter in universal extra dimension models with right-handed neutrinos," arXiv:0705.0934 [hep-ph].

[17] G. Burdman, B. A. Dobrescu and E. Ponton, "Resonances from two universal extra dimensions," Phys. Rev. D **74**, 075008 (2006) [arXiv:hep-ph/0601186], and references therein.

[18] G. Burdman, B. A. Dobrescu and E. Ponton, "Six-dimensional gauge theory on the chiral square," JHEP **0602**, 033 (2006) [arXiv:hep-ph/0506334].

[19] B. A. Dobrescu and E. Pontón, "Chiral compactification on a square," JHEP **0403**, 071 (2004) [arXiv:hep-th/0401032];
M. Hashimoto and D. K. Hong, "Topcolor breaking through boundary conditions," Phys. Rev. D **71**, 056004 (2005) [arXiv:hep-ph/0409223].

[20] E. Ponton and L. Wang, "Radiative effects on the chiral square," JHEP **0611**, 018 (2006) [arXiv:hep-ph/0512304].

[21] B. A. Dobrescu, K. Kong and R. Mahbubani, "Leptons and photons at the LHC: Cascades through spinless adjoints," arXiv:hep-ph/0703231.

[22] M. Srednicki, R. Watkins and K. A. Olive, "Calculations Of Relic Densities In The Early Universe," Nucl. Phys. B **310**, 693 (1988).

[23] K. Griest and D. Seckel, "Three Exceptions In The Calculation Of Relic Abundances," Phys. Rev. D **43**, 3191 (1991).

[24] D. N. Spergel *et al.* [WMAP Collaboration], arXiv:astro-ph/0603449.

[25] The `CalcHEP` files are available at http//theory.fnal.gov/people/kckong/6D.

[26] A. Pukhov *et al.*, "CompHEP: A package for evaluation of Feynman diagrams and integration over multi-particle phase space. User's manual for version 33," arXiv:hep-ph/9908288;
A. Pukhov, "CalcHEP 3.2: MSSM, structure functions, event generation, batchs, and generation of matrix elements for other packages," arXiv:hep-ph/0412191.

[27] G. Belanger, F. Boudjema, A. Pukhov and A. Semenov, "micrOMEGAs2.0: A program to calculate the relic density of dark matter in a generic model," Comput. Phys. Commun. **176**, 367 (2007) [arXiv:hep-ph/0607059].

[28] For a review, see: G. Bertone, D. Hooper and J. Silk, "Particle dark matter: Evidence, candidates and constraints," Phys. Rept. **405**, 279 (2005) [arXiv:hep-ph/0404175].

[29] G. Jungman, M. Kamionkowski and K. Griest, "Supersymmetric dark matter," Phys. Rept. **267**, 195 (1996) [arXiv:hep-ph/9506380].

[30] A. Bottino, F. Donato, N. Fornengo and S. Scopel, "Size of the neutralino nucleon cross-section in the light of a new determination of the pion nucleon sigma term," Astropart. Phys. **18**, 205 (2002) [arXiv:hep-ph/0111229].
J. R. Ellis, K. A. Olive, Y. Santoso and V. C. Spanos, "Update on the direct detection of supersymmetric dark matter," Phys. Rev. D **71**, 095007 (2005) [arXiv:hep-ph/0502001].

[31] J. Angle *et al.* [XENON Collaboration], "First Results from the XENON10 Dark Matter Experiment at the Gran Sasso National Laboratory," arXiv:0706.0039 [astro-ph].

[32] D. S. Akerib *et al.* [CDMS Collaboration], "Limits on spin-independent WIMP nucleon interactions from the two-tower run of the Cryogenic Dark Matter Search," Phys. Rev. Lett. **96**, 011302 (2006) [arXiv:astro-ph/0509259].

[33] Detection sensitivities are summarized at http://dendera.berkeley.edu/plotter/entryform.html

[34] L. Bergstrom, P. Ullio and J. H. Buckley, "Observability of gamma rays from dark matter neutralino annihilations in the Milky Way halo," Astropart. Phys. **9**, 137 (1998) [arXiv:astro-ph/9712318];
V. Berezinsky, A. Bottino and G. Mignola, "High-energy gamma radiation from the galactic center due to neutralino annihilation," Phys. Lett. B **325**, 136 (1994) [arXiv:hep-ph/9402215].

[35] S. Profumo and P. Ullio, "The role of antimatter searches in the hunt for supersymmetric dark matter," JCAP **0407**, 006 (2004) [arXiv:hep-ph/0406018];
D. Hooper and J. Silk, "Searching for dark matter with future cosmic positron experiments," Phys. Rev. D **71**, 083503 (2005) [arXiv:hep-ph/0409104].

[36] L. Bergstrom, J. Edsjo and P. Gondolo, "Indirect detection of dark matter in km-size neutrino telescopes," Phys. Rev. D **58**, 103519 (1998) [arXiv:hep-ph/9806293];
V. D. Barger, F. Halzen, D. Hooper and C. Kao, "Indirect search for neutralino dark matter with high energy neutrinos," Phys. Rev. D **65**, 075022 (2002) [arXiv:hep-ph/0105182].

[37] F. Halzen and D. Hooper, "Prospects for detecting dark matter with neutrino telescopes in light of recent results from direct detection experiments," Phys. Rev. D **73**, 123507 (2006) [arXiv:hep-ph/0510048].

[38] D. Hooper and G. Zaharijas, "Distinguishing supersymmetry from universal extra dimensions or little Higgs models with dark matter experiments," Phys. Rev. D **75**, 035010 (2007) [arXiv:hep-ph/0612137].

[39] R. N. Mohapatra and A. Perez-Lorenzana, "Neutrino mass, proton decay and dark matter in TeV scale universal extra dimension models," Phys. Rev. D **67**, 075015 (2003) [arXiv:hep-ph/0212254];
K. Hsieh, R. N. Mohapatra and S. Nasri, "Mixed dark matter in universal extra dimension models with TeV scale W(R) and Z'," JHEP **0612**, 067 (2006) [arXiv:hep-ph/0610155]; "Dark matter in universal extra dimension models: Kaluza-Klein photon and right-handed neutrino admixture," Phys. Rev. D **74**, 066004 (2006) [arXiv:hep-ph/0604154].